Lymphatic uptake of liposomes after intraperitoneal administration primarily occurs via the diaphragmatic lymphatics and is dependent on liposome surface properties

Given Lee[1,2], Sifei Han[1], Iasmin Inocencio[1], Enyuan Cao[1], Jiwon Hong[3,4], Anthony R.J. Phillips[3,4], John A. Windsor[3,4], Christopher J.H. Porter[1,2], Natalie L. Trevaskis[1]*

[1]Drug Delivery, Disposition and Dynamics, Monash Institute of Pharmaceutical Sciences, Monash University (Parkville Campus), 381 Royal Parade, Parkville, Victoria, Australia 3052

[2]ARC Centre of Excellence in Convergent Bio-Nano Science and Technology, Monash University (Parkville Campus), 399 Royal Parade, Parkville, Victoria, Australia 3052

[3]Applied Surgery and Metabolism Laboratory, School of Biological Sciences and Department of Surgery, University of Auckland, Auckland, New Zealand

[4]Surgical and Translational Research Centre, University of Auckland, Auckland, New Zealand.

*Corresponding author:

Dr Natalie L. Trevaskis

Address: 381 Royal Parade, Parkville, Victoria 3052, Australia

Telephone: +61 3 9903 9708

Fax number: +61 9903 9583

E-mail address: natalie.trevaskis@monash.edu

TABLE OF CONTENTS GRAPHIC

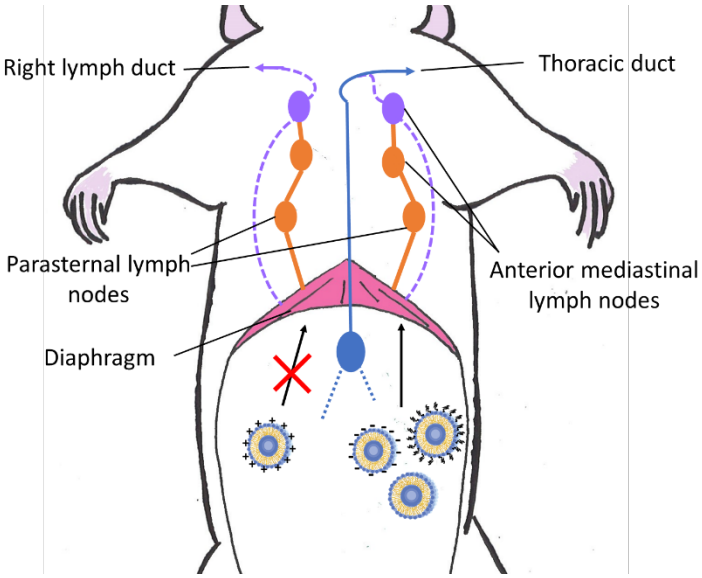

ABSTRACT

Drugs are commonly administered via the intraperitoneal (IP) route to treat localised infections and cancers in patients, and to test drug efficacy and toxicity in pre-clinical studies. Despite this, there remain large gaps in our understanding of drug absorption routes (lymph *vs*. blood) and pharmacokinetics following IP administration. This is particularly true when drugs are administered in complex delivery systems such as liposomes which are the main marketed formulation for several drugs that are administered IP. This study investigated the impact of liposome surface properties (charge and PEGylation) on absorption into lymph and blood, and lymphatic disposition patterns, following IP administration. To achieve this, stable 100-150 nm diameter ^{3}H-dipalmitoyl-phosphatidylcholine (DPPC) and ^{14}C-sucrose radiolabelled liposomes with negative, neutral, or positive surface charge, or a PEGylated surface, were prepared and IP administered to rats. Radiolabel concentrations were measured in lymph, blood and lymph nodes. Lymph was collected from the thoracic lymph duct at either the abdomen (ABD) or the jugular-subclavian junction (JSJ). The lymphatic recovery of the radiolabels was substantially lower after administration in positively charged compared to the neutral, negative or PEGylated liposomes. Radiolabel recovery was substantially greater (up to 18-fold) in thoracic lymph collected at the JSJ when compared to the ABD suggesting that liposomes entered the lymphatics at the diaphragm. Consistent with this, the concentration of the liposome labels was substantially higher (up to 7-fold) in mediastinal than mesenteric lymph nodes. Overall, this study shows how the peritoneal absorption and lymphatic disposition of IP administered drugs can be manipulated through careful selection of the drug delivery system and may thus be optimised to treat localised conditions such as cancers, infections, inflammatory diseases and acute and critical illness.

Keywords: Liposome, Lymphatic uptake, Peritoneum, Intraperitoneal Administration, Drug delivery

Abbreviations: Abdomen (ABD), Area under the plasma concentration curve (AUC), Cholesterol (Chol), Cryogenic Transmission Electron Microscopy (cryo-TEM), Dynamic light scattering (DLS), 1,2-dioleoyl-3-trimethylammonium-propane (DOTAP), Dipalmitoyl-phosphatidylcholine (DPPC), 1,2-distearoyl-sn-glycero-3-phospho-(1'-rac-glycerol), sodium salt (DSPG-Na), N-(Methylpolyoxyethylene oxycarbonyl)-1,2-distearoyl-sn-glycero-3-phosphoethanolamine (DSPE-PEG2000), Intraperitoneal (IP), Jugular-Subclavian Junction (JSJ), Lymph node (LN), Polyethylene glycol (PEG)

INTRODUCTION

The peritoneal cavity is a space that surrounds the internal organs, contains approximately 100 ml of fluid in healthy adults, and is lined by the peritoneum, a serous membrane (Figure 1A)[1, 2]. The peritoneal cavity is utilised to perform peritoneal dialysis in patients with renal failure[3]. Drugs such as antibiotics[4, 5] and chemotherapeutics[6-8] are also delivered via the intraperitoneal (IP) route for the localised treatment of infections and intra-abdominal malignancies (i.e. gynaecological and gastrointestinal cancers)[9]. In these conditions IP administration can provide a treatment advantage over intravenous administration by delivering drug directly to the site of action thus improving therapeutic efficacy and reducing off-target toxicities[4, 5, 9]. IP drug administration is also widely employed in pre-clinical studies in rodents to test drug efficacy and toxicity profiles[10]. Despite the frequent application of the IP route for drug administration, there remain large gaps in our understanding of drug absorption routes and pharmacokinetics following IP administration which in turn impacts our ability to interpret drug efficacy and safety profiles[2]. This is particularly true when drugs are administered IP in complex delivery systems such as liposomes or nanoparticles[2, 9, 11]. Liposomes are the commercially available formulation for several chemotherapeutics (e.g. doxorubicin) administered via the IP route to treat localised cancers[12]. Liposomes and nanoparticles are also commonly employed in pre-clinical studies[10].

Liposomes and nanoparticles are typically absorbed via lymphatic vessels rather than blood vessels following parental extravascular administration (e.g. after subcutaneous, intramuscular or intradermal injection)[13-15]. This contrasts to small molecule drugs which are typically absorbed into blood vessels as the flow rate of blood through capillaries is 100-500 fold higher than the flow rate of lymph fluid[15]. However, the transport of liposomes and nanoparticles across the blood vessel endothelium is impeded by the endothelial tight junctions

[13-15]. In addition, liposomes and nanoparticles may be swept into lymph via the convective flow of interstitial fluid towards the lymphatics[14, 15]. Following IP administration liposomes and nanoparticles are also expected to be absorbed via the lymphatic system[2, 16, 17]. This is because whilst there peritoneum contains a rich supply of blood vessels, the blood vessels are located within a connective tissue layer beneath the mesothelial cells that line the peritoneum[1, 2]. Small molecule drugs can readily diffuse across the mesothelial cell layer and be absorbed into the blood vessels below whereas liposomes and nanoparticles are too large to readily cross either the mesothelial cells or the blood vessel endothelium[1, 2]. On the other hand, uptake into the lymphatic vessels that drain the peritoneum occurs via openings in the peritoneum called stomata (Figure 1B)[1]. Liposomes and nanoparticles may thus be transported from the peritoneum via the stomata and lymphatic system.

The lymphatic system plays essential roles in fluid absorption, immunity and lipid transport, and the lymphatics that drain the peritoneum and internal organs are involved in the development of cancer metastases[18], heart disease[19], metabolic diseases[20, 21], inflammatory diseases[22], and critical illness[23]. IP administration of drugs in liposomes and nanoparticles may thus be utilised to enhance treatment of conditions localised to the peritoneum and/or the draining lymphatics[2]. In this respect, the physical and chemical properties of liposomes and nanoparticles can be manipulated to optimise absorption, lymphatic uptake and therapeutic effect. Particle size is perhaps the most important factor that impacts the peritoneal retention, absorption and lymphatic uptake of liposomes and nanoparticles[2, 16, 24]. Liposomes and nanoparticles that are larger in diameter than the peritoneal stomata are expected to be retained in the peritoneal cavity. Reported diameters of the peritoneal stomata differ across species, however, all are reported within the micron range (e.g. 3.6 μm in mice[25], 2.7 μm in rats[26], 1.2 μm in rabbits[27], and 1.59-1.82 μm in humans[28]). As expected, a study in rats reported similar peritoneal absorption for liposomes with diameters between 48 to 720 nm and thus smaller than

the peritoneal stomata[16]. In contrast, Mirahmadi et al.[11] found that peritoneal retention increased with size following IP administration of liposomes that were 100, 400 or 1000 nm in diameter which was proposed to be a result of sedimentation of the larger liposomes in the peritoneal cavity.

In addition to size, the surface properties of liposomes and nanoparticles can impact peritoneal retention/absorption and are therefore expected to subsequently impact lymphatic uptake after IP administration. The mesothelial cells that line the peritoneum have an anionic surface charge[29, 30]. Positively charged liposomes and nanoparticles are therefore more likely to be retained in the peritoneum and have a lower lymphatic uptake. Indeed, Dadashzadeh et al.[30] and Hirano et al.[17] reported increased peritoneal retention of cationic compared with anionic and neutral radiolabelled liposomes after IP administration. Surface modification of liposomes via the addition of polyethylene glycol (PEG) polymer chains typically increases lymphatic uptake after interstitial administration by reducing interactions with the interstitium as well as reducing opsonisation and uptake by phagocytic cells[15, 31]. However, there is a lack of agreement between studies that have evaluated the effect of adding PEG to the surface of liposomes or nanoparticles on peritoneal retention, with findings that there was an increase[30], no change[32] or decrease[33]. While previous studies have investigated the impact of surface properties of liposomes and nanoparticles on peritoneal retention, little is known about the impact on lymphatic uptake.

The route that is taken from the peritoneum to lymphatic vessels and nodes following IP administration of liposomes and nanoparticles will lead to differential distribution and potentially efficacy and utility of drugs administered IP in these delivery systems. Three separate routes of lymphatic drainage from the peritoneum have been described in animal models (Figure 2)[2]. Whilst lymphatic entry points (i.e. lymphatic stomata) have been identified

in various areas throughout the peritoneum, they appear most abundant on the muscular portion of the diaphragm[2, 33-36]. The first *'parasternal lymphatic' route* from the peritoneum involves uptake into the ventral, diaphragmatic stomata followed by passage through lymphatic vessels that run parallel to the internal thoracic artery, drain into parasternal lymph nodes and flow to mediastinal lymph nodes and then the right lymph duct or thoracic lymph duct[2, 34-37]. The second *'thoracic cavity lymphatic' route* involves uptake via diaphragmatic stomata followed by passage through lymphatic vessels that run along the posterolateral aspect of the thoracic cavity and drain into mediastinal lymph nodes and then the right lymph duct or thoracic lymph duct. The final *'visceral lymphatic' route* involves passage across the peritoneal membrane surrounding the viscera followed by transport via the visceral lymphatics to the cisterna chyli and finally the thoracic lymph duct. The route favoured by liposomes and nanoparticles following IP administration is not known.

There is very limited data available on impact of surface properties of IP drug delivery systems (such as charge and PEGylation) on peritoneal retention and lymphatic uptake, and the preferential route of lymphatic drainage. The aim of the current study was to investigate the impact of surface properties (charge and PEGylation) of liposomes on absorption into lymph and blood following IP administration. Further, the routes of liposome transport through the lymphatics following IP administration were investigated by determining liposome distribution and retention in different lymphatic vessels and lymph nodes. The findings provide new understanding of the impact of liposome surface properties on absorption and lymphatic distribution after IP administration. This will inform the design of delivery systems to optimally treat conditions involving the peritoneum and its draining lymphatics such as cancers, inflammatory diseases, infections and acute and critical illness.

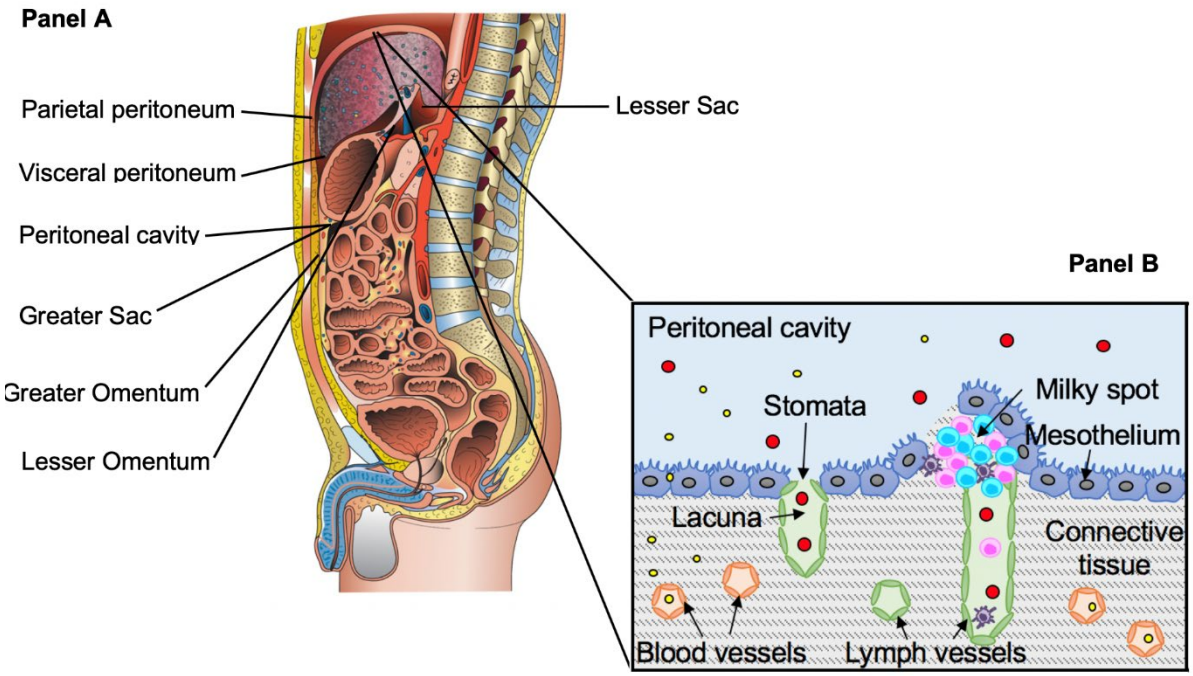

Figure 1. Panel A: A sagittal view of the peritoneal cavity. The peritoneum is divided into two continuous parts: the visceral peritoneum which surrounds the internal organs, and the parietal peritoneum which lines the walls of the abdominal cavity. **Panel B: Diagrammatic representation of the ultrastructure of the parietal peritoneum and the absorption pathways taken by IP administered drugs and delivery systems.** Following IP administration, small molecule drugs (yellow dots) are introduced into the peritoneal fluid and cross the mesothelial cell layer to the connective tissue where they directly drain to the blood vessels. Nano-sized drug delivery systems such as liposomes and nanoparticles (red dots) exit the peritoneal cavity via stomata then enter lymphatic lacuna that drain to the lymphatics[34, 38]. Some stomata are associated with 'milky spots' (aggregates of immune cells such as macrophages and lymphocytes) that are also drained by lymphatic and may be entry points for nano-sized delivery systems[39]. Figure 1 was reproduced from Sarfarazi et al with permission [2].

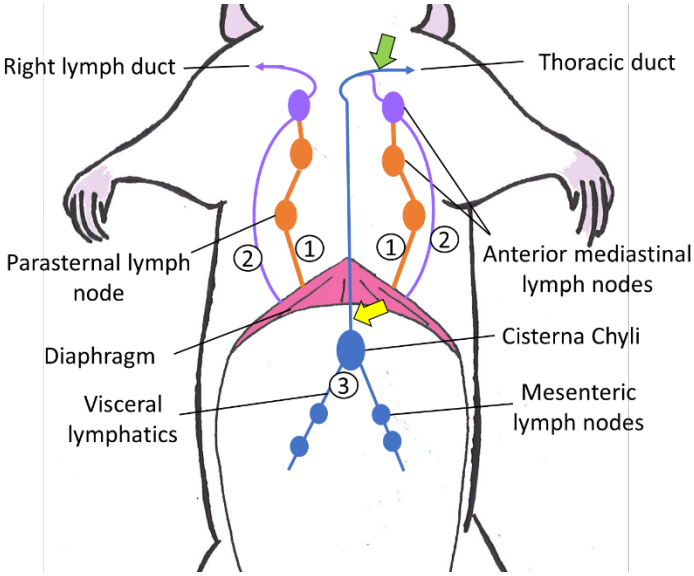

Figure 2. The three routes of lymphatic drainage from the peritoneum. Lymphatic drainage routes from the peritoneum include a parasternal lymphatic pathway (Pathway 1, orange), a thoracic cavity lymphatic pathway (Pathway 2, purple) and a visceral lymphatic pathway (Pathway 3, blue) that join either the thoracic lymphatic duct or right lymphatic duct before connecting to the blood stream. For more detail see Sarfarazi et al [2]. The sites where the thoracic lymph duct was cannulated in the current study are shown with a yellow arrow (abdominal cannulation site) and a green arrow (jugular-subclavian junction (JSJ) cannulation site).

MATERIALS AND METHODS

Materials

Hydrogenated soybean phosphatidylcholine (HSPC), N-(Methylpolyoxyethylene oxycarbonyl)-1,2-distearoyl-sn-glycero-3-phosphoethanolamine (DSPE-PEG2000), and 1,2-distearoyl-sn-glycero-3-phospho-(1'-rac-glycerol), sodium salt (DSPG-Na) were purchased from NOF Corporation (Singapore). 1,2-dioleoyl-3-trimethylammonium-propane, chloride salt (DOTAP) was obtained from Auspep (VIC, Australia). Cholesterol and phosphate buffered saline (PBS) (pH 7.4) were sourced from Sigma-Aldrich (MO, USA). Phosphatidylcholine, L-a-dipalmitoyl [2-palmitoyl-9,10-3H(N)] (^{3}H-DPPC), 250 μCi was purchased from American Radiolabelled Chemicals (MO, USA). Sucrose [^{14}C(U)], 250 μCi and Ultima Gold Scintillation Fluid were ordered from PerkinElmer (MA, USA). Chloroform and methanol were from Merck Millipore (MA, USA).

Experimental design

Rats were IP administered 100-150 nm diameter liposomes with different surface charge and derivatisation (Table 1). Lymph and blood were subsequently collected to quantify absorption and pharmacokinetics (see below for details). Liposomes of 100-150 nm in diameter were employed since this size range is smaller than the peritoneal stomata (i.e. 2.7 μm in rats[26]) which is expected to avoid peritoneal retention[11] and enhance lymph uptake[16]. To determine whether the primary route of lymphatic transport from the peritoneum was via the visceral lymphatic pathway (pathway 3 in Figure 2) or the diaphragmatic lymphatic pathways (pathways 1-2 in Figure 2) the thoracic lymph duct was cannulated at either the abdomen (ABD) or the jugular-subclavian junction (JSJ) (Figure 2). The ABD cannulation site is below the point of entry of diaphragmatic lymph into the thoracic lymph.

Table 1. Experimental groups including liposome type, lipid composition, and thoracic lymph cannulation site

Liposome type	Lipid composition and molar ratio	Thoracic lymph cannulation site
Negative, conventional*	0.15:0.36:0.49 HSPC:DSPG-Na:Chol	JSJ
		ABD
Neutral, conventional	1:1 HSPC:Chol	JSJ
		ABD
Neutral, PEGylated	0.46:0.06:0.49 HSPC:DSPE-PEG2000:Chol	JSJ
		ABD
Positive, conventional	0.18:0.32:0.5 HSPC:DOTAP:Chol	JSJ

Abbreviations: ABD (abdomen), JSJ (jugular-subclavian junction), HSPC (hydrogenated soybean phosphatidylcholine), DSPG-Na (1,2-distearoyl-sn-glycero-3-phospho-(1'-rac-glycerol), sodium salt), DSPE-PEG2000 (N-(Methylpolyoxyethylene oxycarbonyl)-1,2-distearoyl-sn-glycero-3-phosphoethanolamine), DOTAP (1,2-dioleoyl-3-trimethylammonium-propane) and Chol (cholesterol).

*Negative, conventional liposomes were also dosed to all sham group of rats with a cannula inserted into the thoracic lymph duct at the JSJ that had the abdomen opened by laparotomy and then closed consistent with the surgery employed in the ABD thoracic lymph cannulation procedure.

Dual-radiolabelled liposome preparation

Liposomes that were radiolabelled at the lipid bilayer and aqueous core with ^{3}H DPPC and ^{14}C sucrose, respectively, were prepared using the reverse evaporation and extrusion method[40, 41]. Liposomes were dual-radiolabelled to provide greater certainty that the measured radioactivity was indicative of the distribution of intact liposome rather than free radiolabel. Briefly, the lipophilic components of the formulation were first weighed into a 50 ml round bottom flask according to the lipid molar ratios listed in Table 1 at a total concentration of 10 mg lipid per ml. Six ml chloroform was then added to dissolve the lipophilic components. Three µl of ^{3}H DPPC dissolved in ethanol:toluene (1:1 v/v) under argon was added to the mixture to achieve a final radioactivity of 1 µCi/ml of liposome formulation. The contents in the round bottom flask were briefly vortexed, then 3 ml of PBS was added to achieve a volume to volume ratio of 2:1 chloroform to PBS. Subsequently, 240 µl ^{14}C sucrose in ethanol:water (9:1 v/v) was added to achieve a final radioactivity of 8 µCi/ml of liposome formulation. The two-phase system was bath sonicated for 5 minutes at 25ºC with a Soniclean 160HT ultrasonic cleaner (SA, Australia). The round bottom flask was transferred to a rotary evaporator (Rotavapor R-114, Büchi Labortechnik AG, Flawil, Switzerland) to gradually remove the organic solvent under reduced pressure at 60ºC. The temperature of the round bottom flask was maintained using a water bath (Waterbath B-480, Büchi Labortechnik AG, Flawil, Switzerland). The formulation underwent 1-1.5 h of rotary evaporation. After evaporation, the liposomes were downsized by extrusion at 60-70ºC using a mini-extruder set with a heating block (SKU #610000, Avanti Polar Lipids, AL, USA). The formulation was extruded 30 times through three different pore-sized polycarbonate membranes (200 nm, 100 nm, and finally 50 nm from Avanti Polar Lipids, AL, USA). After extrusion, to remove free (i.e. non-liposome associated) radiolabel, the liposome formulations were dialysed with Slide-A-Lyzer Mini

dialysis devices, MWCO 20K (Thermo Fisher Scientific, MA, USA). The dialysate (i.e. PBS) was replaced at 2 h and 4 h after initiation of dialysis to maintain sink conditions.

Liposome characterisation

Liposomes were prepared with a final radioactivity of 1 μCi/ml. Radioactive concentration was confirmed by liquid scintillation counting via addition of 1-2 ml of Ultima Gold Scintillation Fluid (PerkinElmer, MA, USA) to 10 μl of the liposome formulation followed by scintillation counting using a Tri-Carb 2800TR Liquid Scintillation Analyser (PerkinElmer MA, USA). Size, charge and polydispersity of the liposomes were verified by dynamic light scattering (DLS) using a Zetasizer Nano ZS DLS instrument (Malvern Instruments, Worcestershire, UK) with the refractive index set to 1.338. Prior to analysis, the liposome stock was diluted ~10 fold with ultrapure water. Particles within 1 nm to 10 μm diameter were monitored during DLS particle size measurements. A polydispersity index <0.2 was considered an acceptable level of polydispersity.

Size of the liposomes was further verified by cryogenic transmission electron microscopy (cryo-TEM). Sample preparation for cryo-TEM was conducted in a laboratory-built humidity-controlled vitrification system at ~80% humidity and 22°C. 200-mesh copper grids coated with perforated carbon film (Lacey carbon film: ProSciTech, Qld, Australia) were utilized for samples to be imaged by cryo-TEM. The grids were first glow discharged in nitrogen to render them hydrophilic. Four μl of the liposome formulation was pipetted onto the copper grid prior to plunging. After 30 sec adsorption time, the grid was blotted manually using Whatman 541 filter paper, for ~2 sec. Blotting time was optimized for each sample. The grid was then plunged into liquid ethane cooled by liquid nitrogen. Frozen grids were stored in liquid nitrogen until required. The samples were imaged using a Gatan 626 cryoholder (Gatan,

Pleasanton, CA, USA) and a Tecnai 12 Transmission Electron Microscope (FEI, Eindhoven, Netherlands) at an operating voltage of 120 kV. Images were recorded with a FEI Eagle 4k x 4k CCD. Low dose procedures were followed at all times, using an electron dose of 8-10 electrons/Å^2 for all imaging. Size from cryo-TEM images was then determined using Fiji software[42].

The efficiency of incorporation of the ^{3}H DPPC and ^{14}C sucrose radiolabels into the liposomes was determined from the ratio of radioactivity concentration in the formulation before and after dialysis. To determine the radioactivity of the formulations before and after dialysis, a 10 µl aliquot was taken after extrusion and after dialysis and mixed with 1-2 ml of Ultima Gold Scintillation Fluid (PerkinElmer, MA, USA). ^{3}H and ^{14}C radioactivity was then determined by scintillation counting using a Tri-Carb 2800TR Liquid Scintillation Analyser (PerkinElmer MA, USA). The radioactivity after dialysis was divided by the radioactivity after extrusion and multiplied by 100 to determine the proportion of ^{3}H DPPC and ^{14}C sucrose that was associated with the liposome. The remaining radiolabel was assumed to be free in solution.

To determine stability of the ^{3}H DPPC and ^{14}C sucrose liposome radiolabels, 150 µl of the liposome formulations was mixed with 1350 µl of PBS or lymph in 2 ml glass vials. 10 µl of the diluted liposome formulations were immediately mixed with 1-2 ml of Ultima Gold Scintillation Fluid (PerkinElmer, MA, USA) and ^{3}H and ^{14}C radioactivity was measured by scintillation counting using a Tri-Carb 2800TR Liquid Scintillation Analyser (PerkinElmer MA, USA). The liposome and PBS or lymph mixtures were then placed inside a 37^{o}C shaking incubator for 24 h. Samples (250 µl) were taken at a range of time points (0, 2, 4, 8 and 24 h), placed in a polypropylene collection tube with an Amicon Ultra 0.5 ml centrifugal filter unit (3 kDa cut-off, Merck Millipore, MA, USA) and centrifuged for 5 min at 10,000 g to separate liposome associated, and free ^{3}H DPPC and ^{14}C sucrose radiolabel. 10 µl of the filtrate was

mixed with 1-2 ml of Ultima Gold Scintillation Fluid (PerkinElmer, MA, USA) and ^{3}H and ^{14}C radioactivity was measured by scintillation counting using a Tri-Carb 2800TR Liquid Scintillation Analyser (PerkinElmer MA, USA).

Thoracic lymph uptake and plasma pharmacokinetics of liposomes after IP administration to rats

Male SD rats from 280 to 320 g were used in all studies. Studies were approved by the local animal ethics committee and conducted in accordance with the Australian and New Zealand Council for the Care of Animals in Research and Teaching guidelines. Animals were anaesthetised throughout the surgery and sampling period with isoflurane gas delivered via a nose cone. Their temperature was maintained on a 37^{o}C heated pad. Prior to liposome dosing the animals underwent surgery to cannulate the duodenum (for hydration), carotid artery (for blood collection) and thoracic lymph duct (for lymph collection) at either the JSJ or the ABD, as described previously[43, 44]. The rats were then administered 1 ml of liposome formulation IP via a 20G angiocath (BD Insyte 381233 IV catheter, Becton Dickinson, NJ, USA) inserted 2.5 cm into the peritoneal cavity. Following dosing, thoracic lymph was collected continuously for 6 hours into pre-weighed polyethylene tubes containing 10 IU heparin and blood samples were collected every hour for 6 hours into polyethylene tubes containing 3 IU heparin. Whole blood samples were centrifuged at 10,000 g for 5 min to separate plasma. Collected lymph and plasma was stored at -20^{o}C prior to analysis. At the end of the study, animals were euthanised by a 1 ml injection of sodium pentobarbitone (100 mg/ml) via the carotid artery cannula. Immediately after euthanasia, cervical, mediastinal, axillary, and mesenteric lymph nodes were collected and stored at -20^{o}C prior to analysis.

Lymph, blood, and lymph node sample radioactivity analysis

Plasma and lymph samples were prepared for analysis of radiolabel concentrations by mixing 50 µl of plasma or lymph fluid with 2 ml of Ultima Gold scintillation fluid (Perkin Elmer, Boston, USA) in 6 ml polyethylene scintillation vials. Blank plasma and lymph were used to correct for background counts. Samples collected from rats that had the thoracic lymph duct cannulated at the JSJ were also bleached with 200 µl of hydrogen peroxide (H_2O_2, 30% w/v) prior to the addition of scintillation fluid as some contained tracers of the Evans blue dye used to visualise the lymph duct. The quantification of radiolabel concentrations in lymph and plasma was validated by spiking blank plasma and lymph samples with three known concentrations (low, medium and high concentrations of 2, 5 and 9 nCi/ml) of radiolabel. The quantitation method was found to be accurate and precise with less than 10% variability.

Lymph node (LN) samples were prepared for analysis as described previously[45]. Briefly, LNs were solubilised in 0.7 ml of Solvable (Perkin Elmer, Boston, USA) in 6 ml polyethylene scintillation vials overnight at 60ºC. After incubation and cooling to room temperature, 200 µl of H_2O_2 (30% w/v) was added to the LN samples and the samples were left to stand until bubbling ceased. 2 ml of Ultima Gold scintillation fluid was then added, and the samples were kept at 4ºC for 72 hours. Radioactivity of all samples was measured by liquid scintillation counting (LSC-beta, Tri-Carb series, Perkin Elmer, Boston, USA).

Data analysis

Radiolabel concentrations in lymph and plasma are expressed as % dose/ml. Mass transport of radiolabel into lymph during each collection period was calculated from the product of the volume of lymph collected and the radiolabel concentration measured in lymph. Lymph:plasma concentration ratios were determined by dividing the average radiolabel

concentration in lymph for each hourly period by the radiolabel concentration in plasma measured at the end of the hourly collection period. LN recovery and LN radiolabel concentration are expressed as % dose of radiolabel per LN and % dose of radiolabel per gram of LN. LN retention was calculated as the sum of the % dose recovered in LNs through which peritoneal lymph drains (i.e. mesenteric and mediastinal LNs) divided by sum of % dose recovery in the thoracic lymph fluid plus the LNs (i.e. mesenteric and mediastinal).

Statistical methods

Statistical analysis of the data was conducted using GraphPad Prism V7.0. Statistical differences were determined by one-way or two-way ANOVA with Tukey's multiple comparisons test at a significance level of $p=0.05$, unless stated otherwise in the figure legend.

RESULTS

Liposome characterisation and stability

The surface charge and size of the liposomes were verified by DLS and cryo-TEM (Figure 3). Surface charge of the liposomes was as expected; the mean zeta potential of PEGylated, positive, neutral and negative liposomes were -2.3, +26.0, -1.7, and -34.3 mV, respectively (Figure 3, Panel A). The mean liposome sizes were 100-150 nm and 60-90 nm as determined by DLS and cryo-TEM, respectively (Figure 3, Panel B-C and Supplementary Figure 1). The size distribution measured by cryo-TEM compared to DLS may be smaller because the vitrified water layer in cryo-TEM varies in thickness and generally decreases towards the middle of the holes of the copper grid. This can result in the accumulation of larger liposomes at the border which are not imaged and thus leading to an underestimation of the size distribution[46]. All liposome formulations were monodisperse (i.e. the polydispersity index of all formulations assessed via DLS was <0.2). The encapsulation efficiency of ^{3}H DPPC was relatively high for all liposomes (>60%) but significantly greater for the negative liposomes when compared to the positive and PEGylated liposomes (Table 2). Encapsulation efficiency of the ^{14}C sucrose label was generally low for all liposome types (i.e. <10%) (Table 2). Any free label was removed from the liposome formulations by dialysis.

The stability of the radiolabels in the liposome formulations was assessed in PBS and lymph fluid at 37^{o}C over 24 hours since radiolabel may be released from the liposomes during storage prior to dosing or on contact with biological fluids following dosing. Liposome stability in plasma was not investigated as it has been reported previously that liposome stability is similar in lymph and plasma, and the work here is focussed on lymph uptake[16]. All liposomes

were relatively stable over 24 hours in PBS and lymph, with <10% release of both radiolabels into PBS or lymph over 24 hours (Figure 4).

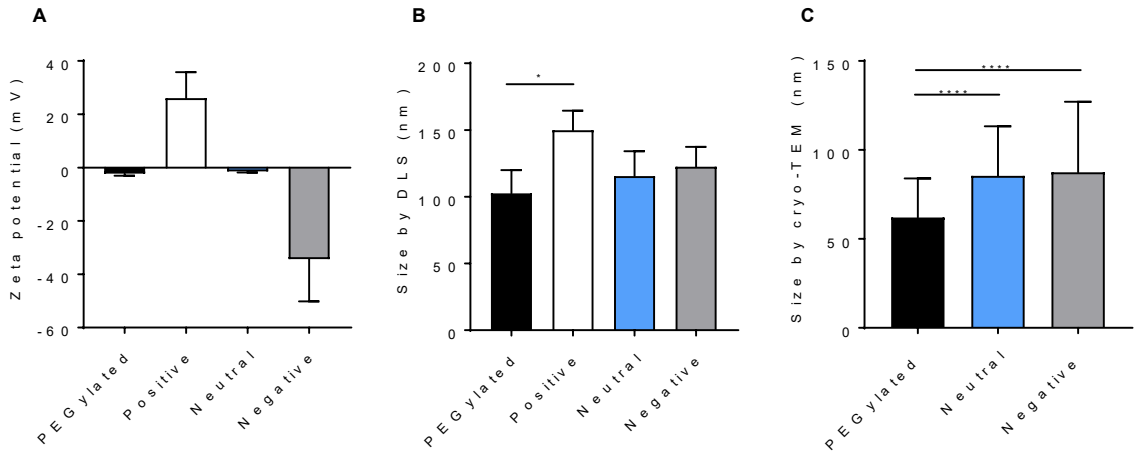

Figure 3. Liposome characterisation. Panel A: Zeta potential and **Panel B:** Particle size of the liposomes were measured by dynamic light scattering (DLS). **Panel C:** Particle size was also confirmed by cryogenic transmission electron microscopy (cryo-TEM). Each formulation type was prepared and characterised in triplicate on three separate days. Data is presented as mean ± SD, n=3. * and **** show statistically significant differences between groups as determined by one-way ANOVA with $p<0.05$ and $p<0.001$, respectively.

Table 2. Liposome characterisation

Liposome type	PEGylated	Negative	Neutral	Positive
Size by DLS (nm)	103 ± 10[a]	123 ± 9	116 ± 11	150 ± 9
Size by Cryo-TEM (nm)	62 ± 22[b]	87 ± 40	86 ± 28	n/a
Polydispersity Index	0.05 ± 0.01	0.07 ± 0.01	0.06 ± 0.01	0.07 ± 0.00
Zeta potential (mV)	-2.3 ± 0.5	-34.3 ± 9.2[c]	-1.4 ± 0.42	+26.0 ± 5.6[e]
Encapsulation efficiency (%) – ^{3}H DPPC	66 ± 6	96 ± 4[d]	81 ± 9	63 ± 2
Encapsulation efficiency (%) – ^{14}C Sucrose	5.7 ± 1.0	9.3 ± 2.0	7.5 ± 0.4	9.6 ± 0.1

DLS data is presented as mean ± SD

Cryo-TEM size is presented as mean ± SD, for 200 particles.

Encapsulation efficiency data is presented as mean ± SD for three formulations prepared on separate days.

[a] Significantly less than positive liposomes ($p<0.05$)

[b] Significantly less than negative and neutral liposomes ($p<0.0001$)

[c] Significantly less than neutral, PEGylated and positive liposomes ($p<0.05$)

[d] Significantly greater than positive and PEGylated liposomes ($p<0.05$)

[e] Significantly greater than neutral, PEGylated, and negative liposomes ($p<0.05$)

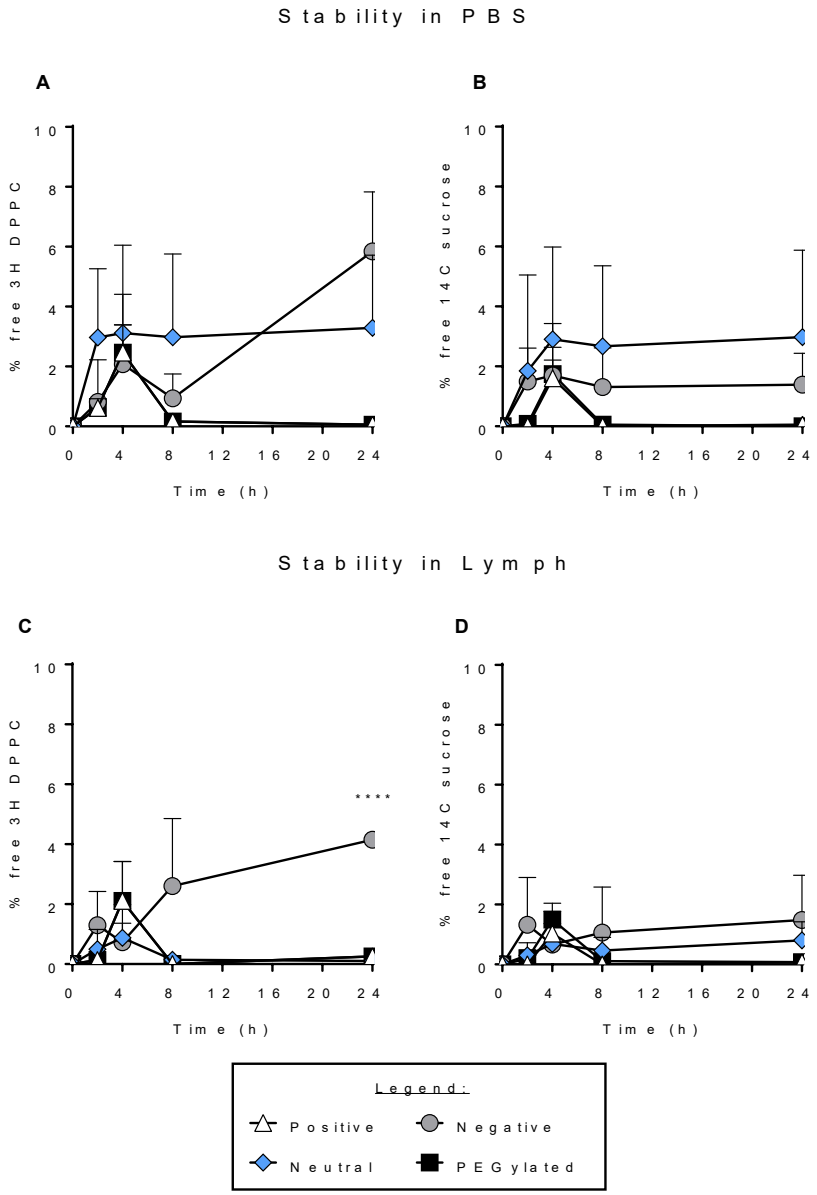

Figure 4. *In vitro* stability of radiolabelled neutral, negative, positive and PEGylated liposomes. Percent release of ^{3}H DPPC (**Panel A**) and ^{14}C sucrose (**Panel B**) from liposomes over time in PBS. Percent release of ^{3}H DPPC (**Panel C**) and ^{14}C sucrose (**Panel D**) from liposomes over time in lymph. One of each formulation was prepared and stability measured in triplicate. Data are shown as mean ± SD. Significant difference to other groups determined from one-way ANOVA: ****$p<0.0001$

Recovery of liposome radiolabels in thoracic lymph collected at the jugular-subclavian junction

The data for ^{3}H DPPC (Figure 5, Panel A and B) and ^{14}C sucrose (Supplementary Figure 2, Panel A and B) cumulative transport and concentration in thoracic lymph collected at the jugular-subclavian junction (JSJ) were very similar. The ratio of ^{3}H DPPC and ^{14}C sucrose in the thoracic lymph collected at the JSJ were also close to one for all except the positive liposomes (Supplementary Figure 2, Panel E). This supports that the negative, neutral and PEGylated liposomes predominantly enter the lymph intact. The ^{3}H DPPC data is primarily presented and discussed here since the data is essentially the same as that for ^{14}C sucrose. The recovery of liposome radiolabels in thoracic lymph collected at the JSJ was relatively high after IP administration of the negative, neutral and PEGylated liposomes (up to 20% of dose administered, Figure 5, Panel A). The radiolabel concentrations in lymph were also generally similar between negative, neutral and PEGylated liposomes where the lymph concentration peaked at 2-3 h post-dose and was relatively consistent until the final time point at 6 h post dose (Figure 5, Panel B). In contrast, the cumulative lymphatic recovery and lymph concentration of radiolabel was substantially lower after IP administration of the positive liposomes (<0.5 % dose and <0.1% dose/ml, respectively) (Figure 5, Panel A and B). The ratio of ^{3}H DPPC and ^{14}C sucrose in the thoracic lymph was substantially less than one after administration in the positive liposomes suggesting that the liposome radiolabels may not enter lymph directly within the positive liposomes.

In general, plasma concentrations of the liposome radiolabels were low when compared to the concentrations in lymph and increased over time up to 6 hours post-dose for all the formulations tested, consistent with a slow rate of absorption (Figure 5, panel C and Supplementary Figure 2, Panel C). Interestingly, the plasma concentrations of the liposome

radiolabels were significantly different after IP administration of the different liposome types. The radiolabel plasma concentrations were significantly greater after dosing the neutral liposomes when compared to the positive and negative liposomes (Figure 5, panel C and Supplementary Figure 2, Panel C). This could reflect either differences in direct absorption of intact liposomes into the blood circulation, differences in clearance of intact liposomes after entering the blood circulation (as has been reported previously[47, 48]) or differences in the released of free radiolabels from the liposomes in the peritoneal cavity followed by uptake into blood. The latter seems most likely since intact liposomes are unlikely to enter the blood circulation efficiently from the peritoneal cavity due to their large size and poor permeability across blood vessels and most of the lymph is being collected/diverted in the animals such that entry into blood cannot occur via the lymph. Further, the lower ratios of ^{3}H DPPC to ^{14}C sucrose seen in plasma (mostly less than one) compared to lymph suggests that the radiolabels entered lymph but not plasma together within the liposomes (Supplementary Figure 2, Panel E and F). The neutral liposomes may thus have lost more radiolabel after IP administration into the peritoneal cavity compared to the other liposome types resulting in higher radiolabel concentrations in plasma. The radiolabel plasma concentrations were particularly low for the positive liposomes suggesting that the poor uptake of radiolabel into both lymph and plasma following administration of these liposomes was due to retention in the peritoneal cavity.

The lymph to plasma concentration ratios of the radiolabels also differed between the liposome groups because the radiolabel lymph concentrations were relatively similar, but the radiolabel plasma concentrations differed. The maximum lymph to plasma concentration ratio of ^{3}H DPPC was 58, 9, 4.5, and 3.1 % dose/ml for negative, PEGylated, positive and neutral liposomes, respectively (Figure 5, panel D). The lymph to plasma concentration ratios were greater than one for all liposomes, supporting that the liposomes directly enter lymph from the IP injection site rather than entering blood first and then extravasating to enter lymph.

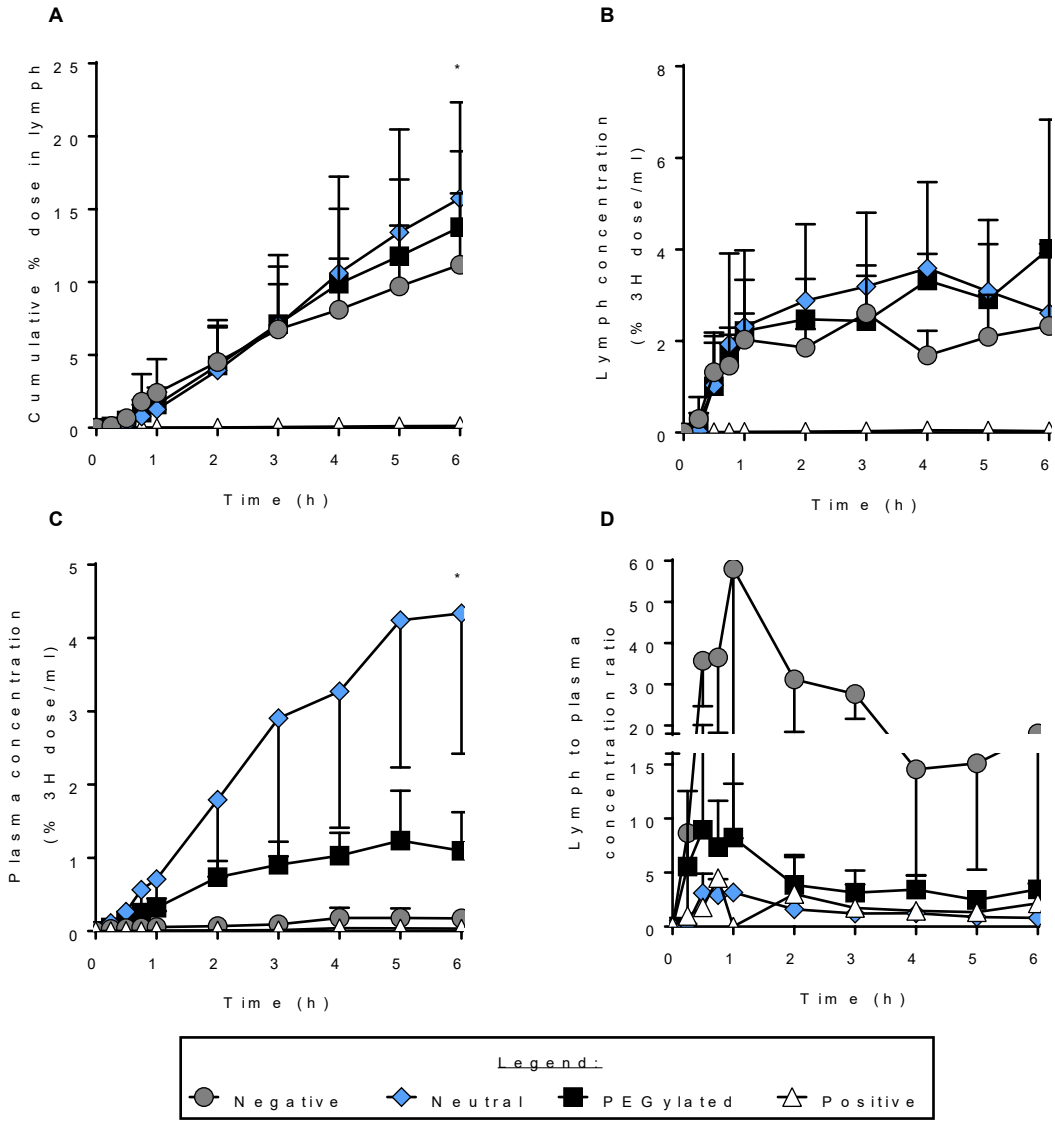

Figure 5. Recovery of liposome ^{3}H DPPC label in the plasma and thoracic lymph collected at the JSJ. Cumulative lymphatic transport of ^{3}H DPPC over time (**Panel A**), concentration of ^{3}H DPPC radiolabel in thoracic lymph (**Panel B**) and plasma (**Panel C**) over time, and the lymph to plasma concentration ratio of ^{3}H DPPC over time (**Panel D**) after IP administration of radiolabelled negative, neutral, positive and PEGylated liposomes to JSJ thoracic lymph cannulated rats. Data is presented as mean ± SD, n=3. Significant difference to other groups

determined from one-way ANOVA: *p<0.05. For panel A, significance applies to positive versus neutral and PEGylated liposomes. For panel C, significance applies to neutral versus negative and positive liposomes.

Recovery of liposome radiolabels in thoracic lymph collected at the abdomen

To investigate the contribution of the visceral lymphatics to lymphatic access of liposomes after IP administration, the lymph uptake experiments with negative, neutral and PEGylated liposomes were repeated with rats where the thoracic lymph duct was cannulated at the abdomen (ABD). Cannulation at this site is below the point of entry of lymph from the diaphragm into the thoracic lymph duct. The lymphatic uptake of the positive liposomes was not determined at this cannulation site as lymph recovery would be very low, consistent with the very low recovery in thoracic lymph collected at the JSJ after IP administration.

The cumulative recovery of liposome radiolabel in thoracic lymph collected at the ABD was <2% of dose for all liposomes after IP administration (Figure 6 and Supplementary Figure 3). The thoracic lymph recovery was thus significantly lower (5-22-fold) after IP administration of the different liposomes to rats with thoracic lymph collected at the ABD when compared to the JSJ (Figure 6, Panel A and Figure 5, Panel A). Lymph concentrations of the liposome radiolabels were also substantially lower in the thoracic lymph collected from the ABD when compared to the JSJ (Figure 6, Panel B and Figure 5, Panel B). The liposomes therefore enter the lymph above the thoracic lymph duct cannulation site at the ABD (Figure 2) suggesting that the major site of lymph uptake is not the visceral lymphatics but rather the diaphragmatic lymphatics.

In the rats where thoracic lymph was collected at the ABD, the radiolabel concentrations in plasma were significantly higher than the lymph concentrations and therefore

the lymph to plasma concentration ratios were low (range from 0.05 to 1.60, Figure 6, Panel C and D). This indicates that the liposome radiolabels enter the blood first before accessing the lymph that flows through to the abdominal thoracic lymph collection site. In the rats with thoracic lymph collected at the ABD, the radiolabels also likely dissociated from the liposomes within the blood prior to accessing lymph as the concentrations of the two radiolabels in lymph and plasma differed from one another (Figure 6 and Supplementary Figure 3). The ^{14}C sucrose concentrations in lymph and plasma peaked at approximately 0.5-0.75 hours post-administration and then declined, whereas the ^{3}H DPPC concentrations in lymph and plasma were steady or increased slowly over the 6 hour collection period (Figure 6 and Supplementary Figure 3). Overall, the results in the ABD thoracic lymph duct cannulated rats demonstrate that the visceral lymphatics are not a primary site of lymphatic access for the IP administered liposomes.

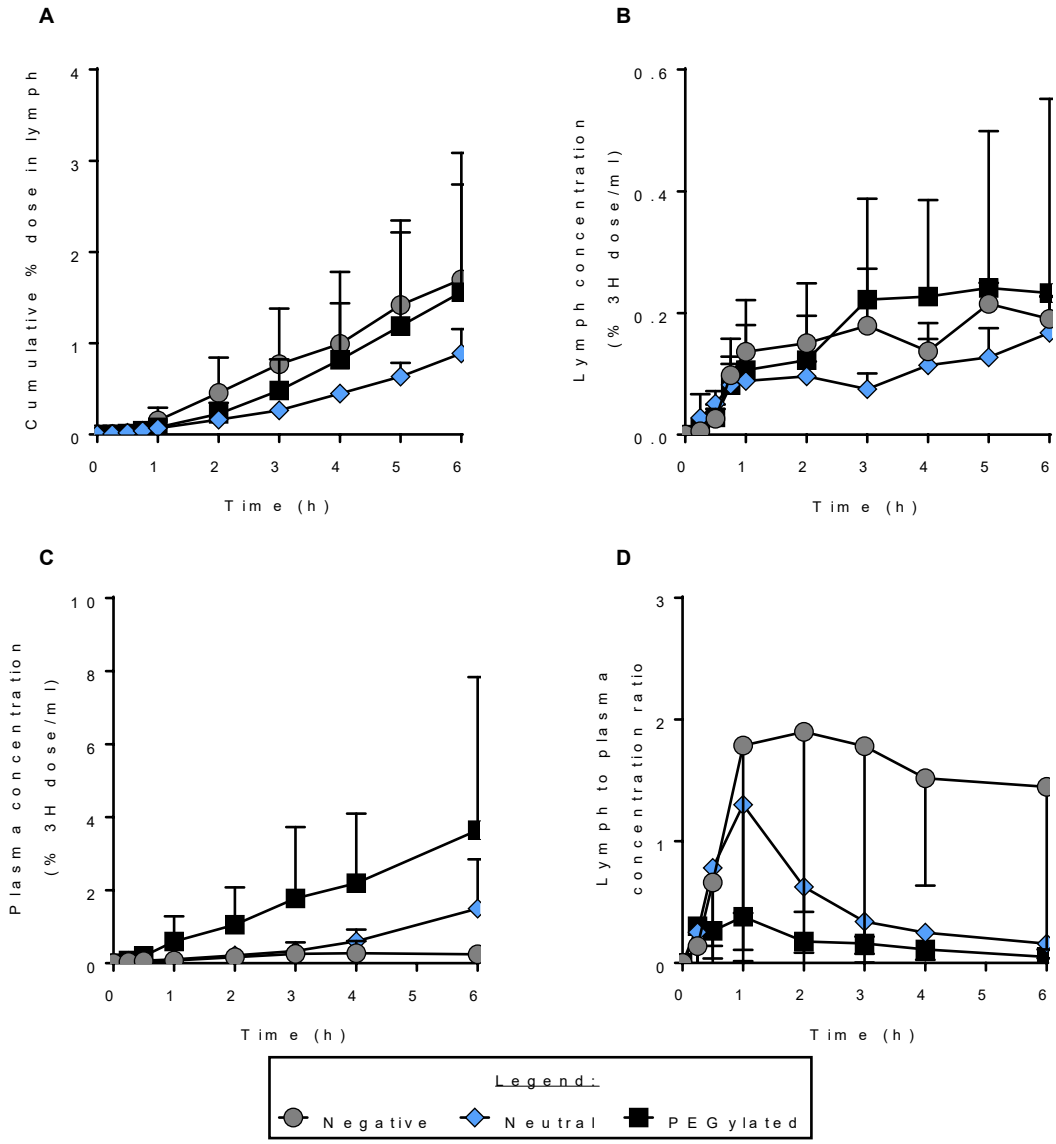

Figure 6. Recovery of liposome ^{3}H DPPC label in thoracic lymph collected at the ABD cannulation site. Cumulative lymphatic transport of ^{3}H DPPC over time (**Panel A**), concentration of ^{3}H DPPC radiolabel in thoracic lymph (**Panel B**) and plasma (**Panel C**) over time, and the lymph to plasma concentration ratio of ^{3}H DPPC over time (**Panel D**) after IP administration of negative, neutral and PEGylated liposomes to ABD thoracic lymph duct cannulated rats. Data is presented as mean ± SD, n=3. No significant difference to other groups was determined by one-way ANOVA.

Verification that the low lymphatic recovery of liposome radiolabels in thoracic lymph collected at the abdomen is not due to surgical disruption of the peritoneum

While the substantial difference in liposome radiolabel recovery in thoracic lymph collected at the ABD and JSJ was likely due to liposomes entering the lymph at the diaphragm, there is the potential that the surgical procedure at the ABD interrupts liposome lymphatic access by damaging the peritoneum. An additional experiment was therefore conducted to confirm that the differences in lymph uptake of liposomes at the ABD versus JSJ thoracic lymph were not the result of the ABD surgery. In this, the abdomen of the rats was opened by laparotomy and closed as per the ABD thoracic lymph cannulation procedure except that the thoracic lymph duct was not cannulated at the ABD and was instead cannulated at the JSJ. Negative liposomes were then IP dosed to the rats and thoracic lymph was collected at the JSJ. The laparotomy did not significantly decrease the mass recovery of the liposome radiolabels in the thoracic lymph collected at the JSJ and only significantly decreased the concentration of the DPPC radiolabel at one time point (Figure 7, Panel A-B and Supplementary Figure 4, Panel A-B). The decrease did not, therefore, account for the decrease in liposome radiolabel recovery in thoracic lymph collected from the ABD when compared to the JSJ. The plasma concentrations of the radiolabels were also relatively similar in the JSJ cannulated rats with or without the laparotomy and the lymph to plasma concentration ratios were substantially higher in JSJ cannulated rats when compared to the ABD cannulated rats (Figure 7, Panel C-D and Supplementary Figure 4, Panel C-D). Therefore, while the laparotomy may have slightly impaired liposome lymphatic uptake, it did not explain the majority of the difference in lymphatic uptake determined at the ABD versus the JSJ.

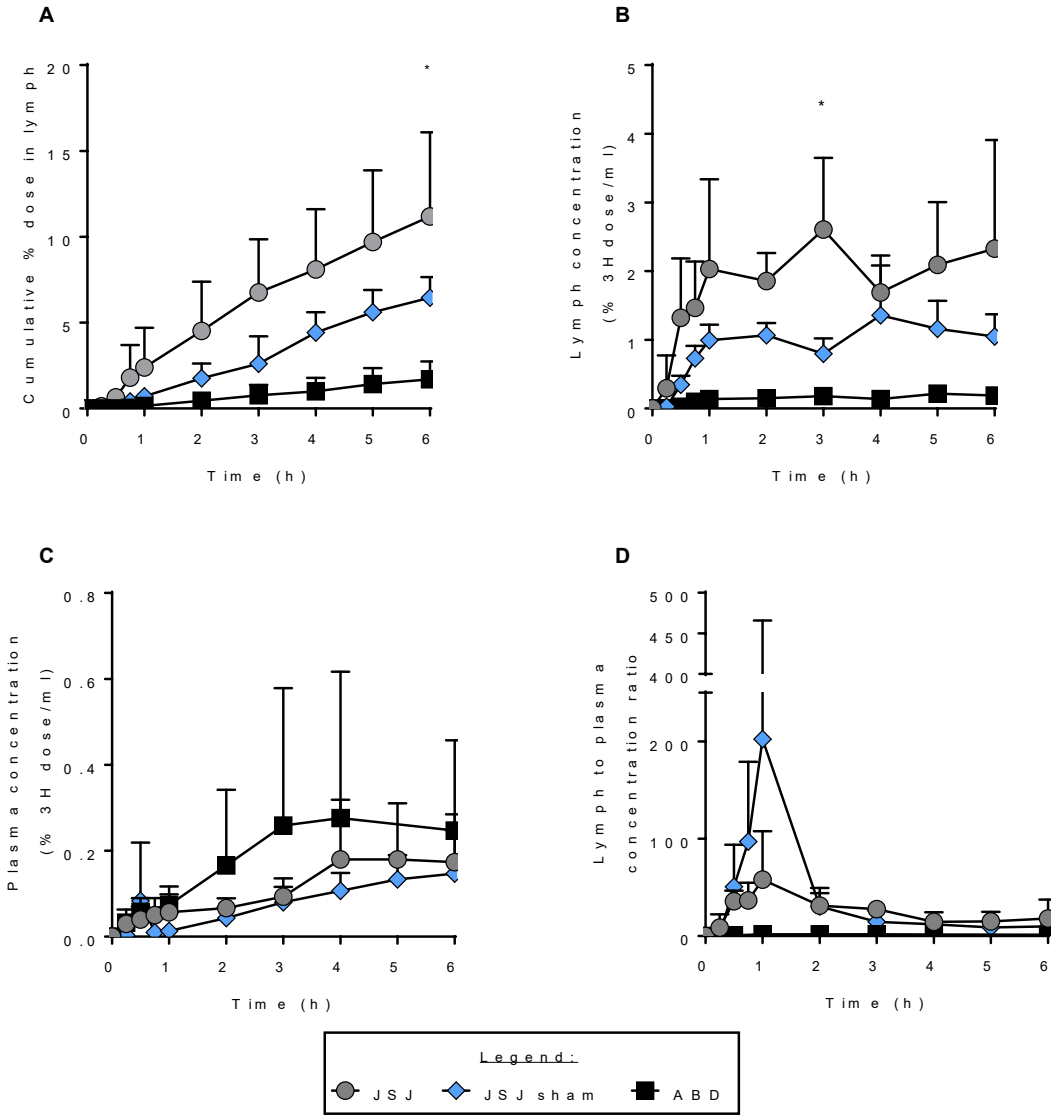

Figure 7. Lymphatic access of negative liposome ^{3}H DPPC label at different lymph duct cannulation sites with and without abdominal surgery (laparotomy). Cumulative lymphatic transport of ^{3}H DPPC over time (**Panel A**) concentration of ^{3}H DPPC radiolabel in thoracic lymph (**Panel B**) and plasma (**Panel C**) over time, and the lymph to plasma concentration ratio of ^{3}H DPPC over time (**Panel D**) following IP administration of negatively charged liposomes to anesthetised rats with the thoracic lymph duct cannulated at the abdomen (ABD), at the jugular-subclavian junction (JSJ) without a laparotomy, or at the JSJ with a laparotomy (i.e. JSJ sham). Data is presented as mean ± SD, n=3. Significant difference to

other groups determined from two-way ANOVA: *p<0.05. For Panel A, significance applies to JSJ versus ABD only. For Panel B significance applies to JSJ versus JSJ sham and ABD.

The lymph node distribution pattern and lymphatic drainage route(s) of liposome radiolabels

Lymph node (LN) retention and distribution patterns of liposome radiolabels provide additional insight into the route of lymphatic transport and the liposome surface properties that impact LN targeting. The mediastinal, cervical, axillary and mesenteric LNs were therefore collected from all the rats at the end of the lymph collection period. The ^{3}H DPPC (Figure 8) and ^{14}C sucrose (Supplementary Figure 5) LN data were very similar (again supporting that the liposomes entered lymph intact) and thus the ^{3}H DPPC data is primarily discussed here. LN recovery data was also obtained for rats with the thoracic lymph duct cannulated at the ABD. The data were similar to the data in the rats with the thoracic lymph duct cannulated at the JSJ and are thus not reported.

The total mass recovery of the liposome radiolabels in the four LN groups was low for all liposomes dosed (<0.1% radiolabel dose) (Figure 8, Panel A), although the concentration of radiolabel in the LNs was relatively high at up to 4800% of the dose per gram (Figure 8, Panel B). Total LN recovery was significantly lower in the rats dosed IP with the positively charged liposomes when compared to negatively charged and neutral liposomes (Figure 8, Panel A). This was consistent with the considerably lower radiolabel recovery in the lymph fluid after IP administration of the positively charged liposomes (Figure 5, Panel A). Radiolabel recovered in the LNs was also significantly less for rats dosed with PEGylated liposomes when compared to neutral conventional liposomes (Figure 8, Panel A and B).

For the liposomes that had substantial lymphatic uptake (i.e. the neutral, negatively charged and PEGylated liposomes), the mediastinal LNs retained the greatest proportion of the liposome radiolabel (Figure 8, Panel B and C). This data suggests that the IP dosed liposomes predominantly access the lymph via the diaphragmatic lymphatics which drain to the mediastinal LNs. This is consistent with the significantly higher recovery of the liposome radiolabels in the thoracic lymph collected from the JSJ (Figure 5, Panel A) when compared to the ABD (Figure 6, Panel A) since the ABD cannulation site is below the point at which the diaphragmatic lymphatics join the thoracic lymph duct whereas the JSJ cannulation site is above it. Recovery in the mediastinal LN was also significantly higher for the neutral liposomes when compared to the PEGylated liposomes (Figure 8, Panel A and B). This is consistent with previous literature where PEGylation is proposed to reduce LN retention by reducing uptake by phagocytic cells[15, 49]. Interestingly, for the positive liposomes, mesenteric LN retention was significantly higher than mediastinal LN retention. This may indicate that the positive liposomes preferentially access the visceral lymphatics from the peritoneal cavity compared to the other liposome types.

To differentiate whether differences in LN recovery of the liposome radiolabels were due to differences in mass transport through the lymphatics and LN or because of enhanced trapping of the radiolabel in the LN, a LN retention ratio was calculated from the mass of radiolabel recovered in the LNs that are expected to receive lymph from the peritoneum (i.e. mediastinal and mesenteric LNs) divided by the mass recovery of the radiolabel in both thoracic lymph and the LNs (Figure 8, Panel C). The LN retention ratio was lower for the PEGylated liposomes when compared to the other liposome types tested. In contrast, the LN retention ratio was significantly greater for positively charged liposomes compared to the other liposome types tested (although absolute retention was low).

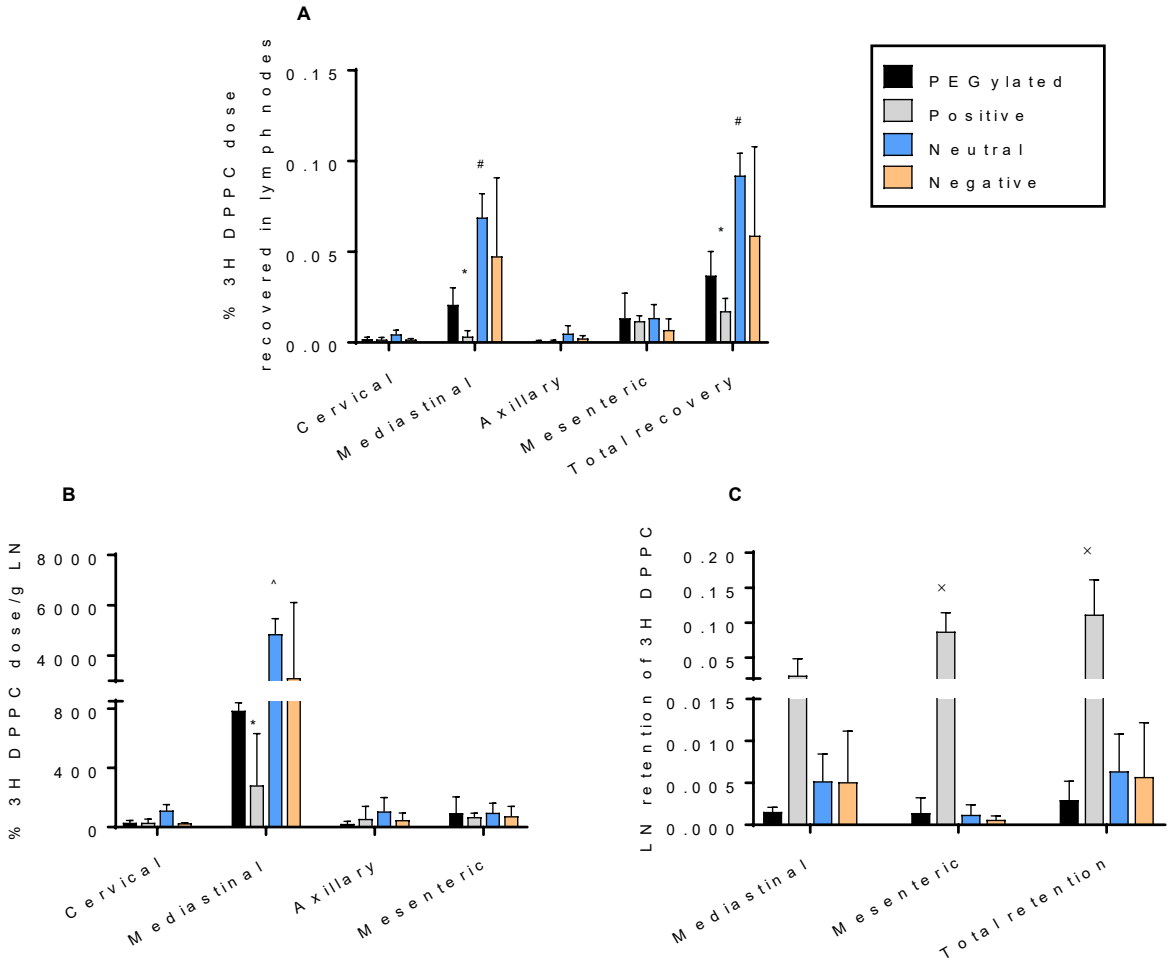

Figure 8. Lymph node (LN) retention and distribution patterns of the liposome ^{3}H DPPC label. Panel A: LN recovery of the liposomes (% dose of ^{3}H DPPC per LN) and **Panel B:** Radiolabel concentration (% ^{3}H DPPC dose per gram of LN) in the cervical, mediastinal, axillary and mesenteric LNs or total LNs (Panel A only), and **Panel C:** LN retention of liposomes (% ratio of ^{3}H DPPC recovered in mediastinal or mesenteric or total LNs relative to total ^{3}H DPPC recovered in LNs plus thoracic lymph). LNs were collected six hours after IP administration of liposomes to anesthetised rats with the thoracic lymph duct cannulated at the JSJ. Data is presented as mean ± SD, n=3. Significant differences to other groups determined from two-way ANOVA with Tukey's multiple comparisons test at a significance level of $p<0.05$: *significant difference between positive versus negative and neutral liposomes,

p<0.05; #significant difference between neutral versus PEGylated liposomes, p<0.05; ^significant difference between neutral versus negative, positive and PEGylated liposomes, p<0.05; ×significant difference between positive versus negative, neutral and PEGylated liposomes, p<0.05

DISCUSSION

The IP route of drug administration is employed in the treatment of intra-abdominal malignancies and peritonitis, and in preclinical studies to test drug efficacy and safety[2, 9]. However, there remain gaps in our understanding of absorption routes (lymph vs. blood) and pharmacokinetics of drugs administered IP in different delivery systems. This impacts our ability to interpret drug efficacy and safety profiles, and to choose the most appropriate delivery system for the desired application. For instance, following IP administration of drugs in liposomes and nanoparticles we expect direct absorption and transport via the lymphatic system[2]. This may be exploited to provide site-specific treatment of conditions involving the lymphatics such as cancer metastases[18], heart disease[19], metabolic diseases[20, 21], inflammatory diseases[22], and critical illness[23]. To this point, however, the impact of liposome surface properties (charge and PEGylation) on absorption into lymph and blood, and lymphatic distribution patterns, following IP administration has not been systematically investigated. Here we therefore show the impact of liposome surface charge and PEGylation on lymphatic uptake, lymph node retention and lymphatic disposition after IP administration. The results inform the design of delivery systems to treat conditions localised to the peritoneum and draining lymphatics.

Liposome surface charge, but not PEGylation, was found to significantly influence lymphatic uptake after IP administration. In particular, the plasma, lymph and LN recovery of

radiolabels was very low after IP administration of positively charged liposomes compared to negative, neutral and PEGylated liposomes. The low lymphatic uptake of the positive liposomes was likely due to retention within the peritoneum due to electrostatic interactions between the positive liposomes and the negatively charged mesothelial cells of the peritoneum[29, 30]. It is also possible that there was some aggregation of the positive liposomes within the peritoneal cavity leading to an increase in particle size, increase in peritoneal retention and reduction in lymphatic uptake. The data is consistent with that of Dadashzadeh et al.[30] who reported that positive surface charge increases peritoneal retention of IP administered liposomes when compared to negative or neutral liposomes in mice. In contrast, Hirano et al. reported similar lymphatic uptake of radiolabels administered with positive, neutral and negative liposomes of 200 nm diameter (all ~10% of dose)[17]. The peritoneal retention of the radiolabels administered with positive liposomes (~71% administered dose retained) was also comparable to the neutral liposomes (~67% of dose retained) but significantly higher than the negative liposomes (~50% dose retained). The similar lymphatic uptake may thus have reflected differences in radiolabel dissociation from the liposomes. In the current study a greater proportion of the liposome radiolabel that entered the lymph was retained within the LNs after administration of the positively charged liposomes compared to the other liposomes tested. This could be attributed to the positive surface charge enhancing particle interaction and uptake by antigen presenting cells either resident within the LN or that traffic to the LN, as shown previously following intraperitoneal[50] and subcutaneous[51, 52] administration of cationic liposomes.

The negative, neutral, and PEGylated liposomes had high and very similar cumulative lymphatic transport and lymph concentrations. PEGylation and negative surface charge therefore did not have a major impact on the lymphatic uptake of liposomes after IP administration. The similar extent of lymphatic uptake for the negative and neutral liposomes

is consistent with previous reports showing similar lymphatic uptake after interstitial administration of negative and neutral liposomes[13, 53]. Both neutral and negative liposomes are expected to have limited charge-charge interactions with the interstitium which predominantly contains negatively charged components such as glycosaminoglycans[54]. In contrast to the similar lymphatic uptake measured for neutral and negative liposomes, the plasma concentrations were significantly higher after administration of the neutral liposomes (Figure 5, Panel C) which may have reflected differences in the absorption and clearance[47, 48] of intact liposomes from the blood but more likely was a result of increased release of free radiolabel from the neutral liposomes after administration into the peritoneal cavity since intact liposomes are unlikely to be well absorbed directly into the blood and the ratios of ^{3}H DPPC to ^{14}C sucrose were low in plasma compared to lymph.

The similarity in lymph uptake for the PEGylated and non-PEGylated neutral liposomes after IP administration is in contrast with previous studies where PEGylation of nanocarriers enhanced lymphatic uptake after interstitial administration[31, 55-57]. This is likely due to differences in the 'barriers' that influence access. Access to the lymphatics from the peritoneal cavity can occur directly via entry into the lymphatic stomata whereas following subcutaneous administration liposome transport through and interaction with the interstitial tissue is required prior to lymphatic access[2]. No study has previously directly assessed the impact of nanocarrier PEGylation on thoracic lymph uptake following IP administration. However, a limited number of studies have investigated the impact of PEGylation on nanocarrier retention in the peritoneal cavity after IP administration which will influence the extent of uptake into lymph and blood. The results from these studies have been contradictory and suggested that PEGylation may reduce[30], increase[33] or have no effect[32] on peritoneal retention. Accurate measurement of drug delivery system retention within the peritoneal cavity is, however, technically difficult. Also, the size and composition of the liposomes differed

across studies which may have impacted retention. In the study by Singhania et al.[33] it was suggested that PEGylated lipoplexes display enhanced tumour localization when compared to non-PEGylated lipoplexes following IP administration due to enhanced uptake into the diaphragmatic lymphatics. However, lymphatic uptake was not measured and was instead inferred from enhanced tumour localization which may be a result of a range of factors that influence lipoplex distribution and clearance, in addition to lymphatic uptake. For example, tumour uptake may be enhanced with PEGylation due to reduced uptake and clearance by the mononuclear phagocyte system in the spleen and liver[31, 58, 59].

While in the current study PEGylation did not appear to impact lymph uptake, the LN recovery of liposome radiolabel was significantly lower after IP administration of the PEGylated liposomes when compared to the neutral non-PEGylated liposomes. This is consistent with previous studies showing that PEGylation inhibits liposome opsonisation and phagocytosis by antigen presenting cells either resident in LNs or that migrate to LNs, and thus reduces LN retention of liposomes after subcutaneous administration[15, 57, 60].

The current study also shed new light on the drainage route of liposomes after IP administration. The negative, neutral and PEGylated liposomes appeared to enter the thoracic lymph above the ABD thoracic lymph cannulation site as the lymphatic uptake and lymph concentration of liposome radiolabels was very low in thoracic lymph collected at the ABD but substantially greater in thoracic lymph collected from the JSJ. In addition, the majority of liposome radiolabel recovered in LNs was found in the mediastinal LNs for the negative, neutral and PEGylated liposomes. This is consistent with previous studies that have suggested that the major lymphatic drainage route from the peritoneal cavity is via the diaphragmatic lymphatics that commence at the stomata in the parietal peritoneum[28, 34, 35]. However, these previous studies have examined uptake of non-drug related materials (e.g. India Ink dye[61],

erythrocytes and albumin[62-65], graphite particles[36, 66] or radiocontrast agents[35]). In contrast, a recent study suggested that 20 nm diameter quantum dots are predominantly cleared from the peritoneal cavity via the visceral lymphatics after IP administration[67]. Interestingly, the positively charged liposomes in the current study seemed to have proportionally greater uptake via the visceral lymphatics. For the IP administered positive liposomes, retention in mesenteric LNs was significantly greater ($p<0.05$) than in mediastinal LNs. In contrast, relative LN retention was greater in the mediastinal LNs after administration of the negative and neutral liposomes. In summary, the results suggest that the main lymphatic drainage route/s for the negative, neutral and PEGylated liposomes is via uptake into the diaphragmatic lymphatics that flow to the mediastinal lymph nodes (i.e. route 1 and/or 2 on Figure 2) whereas positively charged liposomes have low lymphatic uptake but the proportion that enters lymph may be drained more via the visceral lymphatic route (i.e. route 3 on Figure 2). Carrier properties may thus influence the lymphatic drainage route.

Liposome transport to the right lymph duct following IP administration was not directly quantified here. The diaphragmatic lymphatics on the right hand side may join the right lymphatic duct. Therefore, it is possible that some of the liposome radiolabel was transported into the blood circulation from the peritoneal cavity via the right lymphatic duct. While it would be ideal to have measured uptake into the right lymphatic duct, it has not been possible to cannulated this duct in rats and rarely in dogs and pigs[68, 69]. The relative contribution of transport via the thoracic duct and right lymphatic duct to the total systemic exposure of the liposome radiolabels after IP administration can be estimated from the proportional reduction in the radiolabel plasma exposure (AUC of the plasma concentration vs. time profile) in rats with thoracic lymph collected at the JSJ versus ABD (Supplementary Table 1). From this calculation using the data for the negatively charged and PEGylated liposomes, ~60% of the systemic exposure is estimated to be contributed by transport via the thoracic lymph duct. The

remaining 40% of the systemic exposure is either contributed by direct access of radiolabel to the blood circulation from the peritoneal cavity or transport via the right lymphatic duct. Interestingly, previous studies have suggested that ~70-80% of the fluid from the peritoneal cavity is returned to the venous circulation via the right lymph duct and that ~20-30% is via the thoracic lymph duct[35, 64, 65, 70, 71]. However, it should be noted that in these studies, drainage to the right lymphatic duct was either qualitatively assessed via visualisation of drainage of dyes/radiocontrast agents or estimated indirectly via measurement of parasternal LN uptake. Additionally, the proportional drainage of fluid via the right and thoracic lymphatic ducts may differ to the transport of drug carriers such as liposomes. Overall, the results from our study suggest that proportionally more transport of liposomes occurs via the thoracic lymph duct when compared to the right lymphatic duct following IP administration.

Conclusion

This study demonstrates the impact of surface charge and PEGylation on liposome absorption into lymph and blood, and lymphatic distribution, after IP administration. IP administration in 100-150 nm diameter neutral, negative and PEGylated liposomes results in significant lymphatic uptake. The lymphatic uptake of the neutral, negative and PEGylated liposomes appears to occur at the diaphragmatic lymphatics and from here the liposomes flow to the mediastinal lymph nodes before entering the thoracic lymph duct. In contrast, IP administration in positively charged liposomes results in minimal lymphatic uptake, most likely due to retention in the peritoneum. However, of the positive liposomes that are absorbed into lymph, more are retained within the lymph nodes, particularly in the mesenteric lymph nodes. Conversely PEGylated liposomes are the least retained in the lymph nodes. In this way, IP administration of drugs in neutral or negative liposomes may facilitate access to and treatment of conditions involving the lymphatic vessels and nodes that drain the diaphragm. In

contrast, IP administration of drugs in PEGylated liposomes may be more useful to access treatment targets within the lymph fluid or blood circulation. Overall, the data demonstrates that IP administration in nanocarriers such as liposomes can facilitate drug delivery to therapeutic targets within the lymphatics that drain the peritoneum and internal organs. This may provide a treatment benefit for conditions that are localised to the peritoneum and draining lymphatics such as infections, cancers, inflammatory and metabolic diseases.

Acknowledgements

This grant was financially supported by New Zealand Health Research Council Project Grant 16-036.

Supporting information

Supporting information available online includes: Liposome characterisation by Cryo-TEM (Figure S1), Lymph and plasma pharmacokinetics of ^{14}C-sucrose liposome radiolabel in rats with the thoracic lymph duct cannulated at the jugular subclavian junction (Figure S2) or abdomen (Figure S3), Lymphatic access of negative liposome ^{14}C sucrose label at different lymph duct cannulation sites with and without abdominal surgery (laparotomy) (Figure S4), Lymph node (LN) retention and distribution patterns of the liposome ^{14}C sucrose label (Figure S5), Calculation of approximate % contribution of lymphatic transport via the thoracic lymph duct to the systemic exposure (Table S1)

References

1. Mactier, R. A.; Khanna, R., Peritoneal lymphatics. In *Textbook of Peritoneal Dialysis*, Gokal, R.; Khanna, R.; Krediet, R. T.; Nolph, K. D., Eds. Springer Netherlands: Dordrecht, 2000; pp 173-192.
2. Sarfarazi, A.; Lee, G.; Mirjalili, S. A.; Phillips, A. R. J.; Windsor, J. A.; Trevaskis, N. L. Therapeutic delivery to the peritoneal lymphatics: Current understanding, potential

treatment benefits and future prospects. *International Journal of Pharmaceutics* **2019,** *567*, 118456.
3. Davies, S. J. Peritoneal dialysis—current status and future challenges. *Nature Reviews Nephrology* **2013,** *9*, 399.
4. Bennett-jones, D.; Wass, V.; Mawson, P.; Taube, D.; Neild, G.; Ogg, C.; Cameron, j. S.; Williams, D. G. A comparison of intraperitoneal and intravenous/oral antibiotics in CAPD peritonitis. *Peritoneal Dialysis International* **1987,** *7*, (1), 31-33.
5. Li, P. K.-T.; Szeto, C. C.; Piraino, B.; de Arteaga, J.; Fan, S.; Figueiredo, A. E.; Fish, D. N.; Goffin, E.; Kim, Y.-L.; Salzer, W.; Struijk, D. G.; Teitelbaum, I.; Johnson, D. W. ISPD Peritonitis Recommendations: 2016 Update on Prevention and Treatment. *Peritoneal Dialysis International* **2016,** *36*, (5), 481-508.
6. Markman, M.; Kelsen, D. Efficacy of cisplatin-based intraperitoneal chemotherapy as treatment of malignant peritoneal mesothelioma. *Journal of Cancer Research and Clinical Oncology* **1992,** *118*, (7), 547-550.
7. Jaaback, K.; Johnson, N.; Lawrie, T. A. Intraperitoneal chemotherapy for the initial management of primary epithelial ovarian cancer. *Cochrane Database of Systematic Reviews* **2016**, (1).
8. Yan, T. D.; Black, D.; Sugarbaker, P. H.; Zhu, J.; Yonemura, Y.; Petrou, G.; Morris, D. L. A Systematic Review and Meta-analysis of the Randomized Controlled Trials on Adjuvant Intraperitoneal Chemotherapy for Resectable Gastric Cancer. *Annals of Surgical Oncology* **2007,** *14*, (10), 2702-2713.
9. Kunal, C.; Shadi, H.; Ravi, N.; Chris, P. Intraperitoneal Drug Therapy: An Advantage. *Current Clinical Pharmacology* **2010,** *5*, (2), 82-88.
10. Williams, H. D.; Trevaskis, N. L.; Charman, S. A.; Shanker, R. M.; Charman, W. N.; Pouton, C. W.; Porter, C. J. Strategies to address low drug solubility in discovery and development. *Pharmacological reviews* **2013,** *65*, (1), 315-499.
11. Mirahmadi, N.; Babaei, M.; Vali, A.; Dadashzadeh, S. Effect of liposome size on peritoneal retention and organ distribution after intraperitoneal injection in mice. *International Journal of Pharmaceutics* **2010,** *383*, (1), 7-13.
12. Salvatorelli, E.; De Tursi, M.; Menna, P.; Carella, C.; Massari, R.; Colasante, A.; Iacobelli, S.; Minotti, G. Pharmacokinetics of Pegylated Liposomal Doxorubicin Administered by Intraoperative Hyperthermic Intraperitoneal Chemotherapy to Patients with Advanced Ovarian Cancer and Peritoneal Carcinomatosis. *Drug Metabolism and Disposition* **2012,** *40*, (12), 2365-2373.
13. Oussoren, C.; Zuidema, J.; Crommelin, D.; Storm, G. Lymphatic uptake and biodistribution of liposomes after subcutaneous injection.: II. Influence of liposomal size, lipid composition and lipid dose. *Biochimica et Biophysica Acta (BBA)-Biomembranes* **1997,** *1328*, (2), 261-272.
14. Reddy, S. T.; Van Der Vlies, A. J.; Simeoni, E.; Angeli, V.; Randolph, G. J.; O'Neil, C. P.; Lee, L. K.; Swartz, M. A.; Hubbell, J. A. Exploiting lymphatic transport and complement activation in nanoparticle vaccines. *Nature Biotechnology* **2007,** *25*, (10), 1159.
15. Trevaskis, N. L.; Kaminskas, L. M.; Porter, C. J. From sewer to saviour [mdash] targeting the lymphatic system to promote drug exposure and activity. *Nature Reviews Drug Discovery* **2015**.
16. Hirano, K.; Anthony Hunt, C. Lymphatic transport of liposome-encapsulated agents: Effects of liposome size following intraperitoneal administration. *Journal of Pharmaceutical Sciences* **1985,** *74*, (9), 915-921.
17. Hirano, K.; Hunt, C. A.; Strubbe, A.; MacGregor, R. Lymphatic Transport of Liposome-Encapsulated Drugs Following Intraperitoneal Administration – Effect of Lipid Composition. *Pharmaceutical Research* **1985,** *2*, (6), 271-278.

18. Karaman, S.; Detmar, M. Mechanisms of lymphatic metastasis. *The Journal of Clinical Investigation* **2014,** *124*, (3), 922-928.
19. Brakenhielm, E.; Alitalo, K. Cardiac lymphatics in health and disease. *Nature Reviews Cardiology* **2019,** *16*, (1), 56-68.
20. Martel, C.; Li, W.; Fulp, B.; Platt, A. M.; Gautier, E. L.; Westerterp, M.; Bittman, R.; Tall, A. R.; Chen, S.-H.; Thomas, M. J. Lymphatic vasculature mediates macrophage reverse cholesterol transport in mice. *The Journal of Clinical Investigation* **2013,** *123*, (4), 1571-1579.
21. Escobedo, N.; Oliver, G. The Lymphatic Vasculature: Its Role in Adipose Metabolism and Obesity. *Cell Metabolism.* **2017,** *26*, (4), 598-609.
22. Schwager, S.; Detmar, M. Inflammation and Lymphatic Function. *Frontiers in Immunology* **2019,** *10*, (308).
23. Windsor, J. A.; Escott, A.; Brown, L.; Phillips, A. R. Novel strategies for the treatment of acute pancreatitis based on the determinants of severity. *Journal of Gastroenterology and Hepatology* **2017,** *32*, (11), 1796-1803.
24. Forster, V.; Signorell, R. D.; Roveri, M.; Leroux, J.-C. Liposome-supported peritoneal dialysis for detoxification of drugs and endogenous metabolites. *Science Translational Medicine* **2014,** *6*, (258), 258ra141-258ra141.
25. Tsai, M.; Lu, Z.; Wang, J.; Yeh, T.-K.; Wientjes, M. G.; Au, J. L. S. Effects of carrier on disposition and antitumour activity of intraperitoneal paclitaxel. *Pharmaceutical Research* **2007,** *24*, (9), 1691-1701.
26. Michailova, K. N. Postinflammatory changes of the diaphragmatic stomata. *Annals of Anatomy-Anatomischer Anzeiger* **2001,** *183*, (4), 309-317.
27. Negrini, D.; Mukenge, S.; Del Fabbro, M.; Gonano, C.; Miserocchi, G. Distribution of diaphragmatic lymphatic stomata. *Journal of Applied Physiology* **1991,** *70*, (4), 1544-1549.
28. Ji-Chang, L.; Shou-Min, Y. Study on the infrastructure of the Peritoneal Stomata in Humans. *Cells Tissues Organs* **1991,** *141*, (1), 26-30.
29. Dakwar, G. R.; Shariati, M.; Willaert, W.; Ceelen, W.; De Smedt, S. C.; Remaut, K. Nanomedicine-based intraperitoneal therapy for the treatment of peritoneal carcinomatosis—Mission possible? *Advanced Drug Delivery Reviews* **2017,** *108*, 13-24.
30. Dadashzadeh, S.; Mirahmadi, N.; Babaei, M.; Vali, A. Peritoneal retention of liposomes: Effects of lipid composition, PEG coating and liposome charge. *Journal of Controlled Release* **2010,** *148*, (2), 177-186.
31. Ryan, G. M.; Kaminskas, L. M.; Porter, C. J. Nano-chemotherapeutics: Maximising lymphatic drug exposure to improve the treatment of lymph-metastatic cancers. *Journal of Controlled Release* **2014,** *193*, 241-256.
32. Sadzuka, Y.; Hirota, S.; Sonobe, T. Intraperitoneal administration of doxorubicin encapsulating liposomes against peritoneal dissemination. *Toxicology Letters* **2000,** *116*, (1), 51-59.
33. Singhania, A.; Wu, S. Y.; McMillan, N. A. Effective delivery of PEGylated siRNA-containing lipoplexes to extraperitoneal tumours following intraperitoneal administration. *Journal of Drug Delivery* **2011,** *2011*.
34. Abu-Hijleh, M. F.; Habbal, O. A.; Moqattash, S. T. The role of the diaphragm in lymphatic absorption from the peritoneal cavity. *Journal of Anatomy* **1995,** *186*, (Pt 3), 453.
35. Olin, T.; Saldeen, T. The lymphatic pathways from the peritoneal cavity: a lymphangiographic study in the rat. *Cancer Research* **1964,** *24*, (10), 1700-1711.
36. Higgins, G. M.; Graham, A. S. Lymphatic drainage from the peritoneal cavity in the dog. *Archives of Surgery* **1929,** *19*, (3), 453-465.
37. Courtice, F.; Steinbeck, A. Absorption of protein from the peritoneal cavity. *The Journal of physiology* **1951,** *114*, (3), 336-355.

38. Wang, Z. B.; Li, M.; Li, J. C. Recent advances in the research of lymphatic stomata. *The Anatomical Record: Advances in Integrative Anatomy and Evolutionary Biology* **2010,** *293*, (5), 754-761.
39. Mebius, R. E. Lymphoid Organs for Peritoneal Cavity Immune Response: Milky Spots. *Immunity* **2009,** *30*, (5), 670-672.
40. Watwe, R. M.; Bellare, J. R. Manufacture of liposomes: a review. *Current Science* **1995**, 715-724.
41. Szoka, F.; Olson, F.; Heath, T.; Vail, W.; Mayhew, E.; Papahadjopoulos, D. Preparation of unilamellar liposomes of intermediate size (0.1–0.2 μm) by a combination of reverse phase evaporation and extrusion through polycarbonate membranes. *Biochimica et Biophysica Acta (BBA)-Biomembranes* **1980,** *601*, 559-571.
42. Schindelin, J.; Arganda-Carreras, I.; Frise, E.; Kaynig, V.; Longair, M.; Pietzsch, T.; Preibisch, S.; Rueden, C.; Saalfeld, S.; Schmid, B. Fiji: an open-source platform for biological-image analysis. *Nature Methods* **2012,** *9*, (7), 676.
43. Boyd, M.; Risovic, V.; Jull, P.; Choo, E.; Wasan, K. M. A stepwise surgical procedure to investigate the lymphatic transport of lipid-based oral drug formulations: cannulation of the mesenteric and thoracic lymph ducts within the rat. *Journal of Pharmacological and Toxicological Methods* **2004,** *49*, (2), 115-120.
44. Yadav, P.; McLeod, V. M.; Nowell, C. J.; Selby, L. I.; Johnston, A. P. R.; Kaminskas, L. M.; Trevaskis, N. L. Distribution of therapeutic proteins into thoracic lymph after intravenous administration is protein size-dependent and primarily occurs within the liver and mesentery. *Journal of Controlled Release* **2018,** *272*, 17-28.
45. Boyd, B. J.; Kaminskas, L. M.; Karellas, P.; Krippner, G.; Lessene, R.; Porter, C. J. Cationic poly-L-lysine dendrimers: pharmacokinetics, biodistribution, and evidence for metabolism and bioresorption after intravenous administration to rats. *Molecular Pharmaceutics* **2006,** *3*, (5), 614-627.
46. Egelhaaf, S.; Wehrli, E.; Müller, M.; Adrian, M.; Schurtenberger, P. Determination of the size distribution of lecithin liposomes: a comparative study using freeze fracture, cryoelectron microscopy and dynamic light scattering. *Journal of Microscopy* **1996,** *184*, (3), 214-228.
47. Gabizon, A.; Papahadjopoulos, D. The role of surface charge and hydrophilic groups on liposome clearance in vivo. *Biochimica et Biophysica Acta (BBA) - Biomembranes* **1992,** *1103*, (1), 94-100.
48. Levchenko, T. S.; Rammohan, R.; Lukyanov, A. N.; Whiteman, K. R.; Torchilin, V. P. Liposome clearance in mice: the effect of a separate and combined presence of surface charge and polymer coating. *International Journal of Pharmaceutics* **2002,** *240*, (1), 95-102.
49. Jiang, H.; Wang, Q.; Sun, X. Lymph node targeting strategies to improve vaccination efficacy. *Journal of Controlled Release* **2017,** *267*, 47-56.
50. Schmidt, S. T.; Khadke, S.; Korsholm, K. S.; Perrie, Y.; Rades, T.; Andersen, P.; Foged, C.; Christensen, D. The administration route is decisive for the ability of the vaccine adjuvant CAF09 to induce antigen-specific CD8+ T-cell responses: The immunological consequences of the biodistribution profile. *Journal of Controlled Release* **2016,** *239*, 107-117.
51. Zeng, Q.; Jiang, H.; Wang, T.; Zhang, Z.; Gong, T.; Sun, X. Cationic micelle delivery of Trp2 peptide for efficient lymphatic draining and enhanced cytotoxic T-lymphocyte responses. *Journal of Controlled Release* **2015,** *200*, 1-12.
52. Kim, C.; Han, J. Lymphatic delivery and pharmacokinetics of methotrexate after intramuscular injection of differently charged liposome-entrapped methotrexate to rats. *Journal of Microencapsulation* **1995,** *12*, (4), 437-446.
53. Oussoren, C.; Velinova, M.; Scherphof, G.; van der Want, J. J.; van Rooijen, N.; Storm, G. Lymphatic uptake and biodistribution of liposomes after subcutaneous injection: IV. Fate

of liposomes in regional lymph nodes. *Biochimica et Biophysica Acta (BBA) - Biomembranes* **1998,** *1370*, (2), 259-272.
54. Stylianopoulos, T.; Poh, M.-Z.; Insin, N.; Bawendi, M. G.; Fukumura, D.; Munn, Lance L.; Jain, R. K. Diffusion of Particles in the Extracellular Matrix: The Effect of Repulsive Electrostatic Interactions. *Biophysical Journal* **2010,** *99*, (5), 1342-1349.
55. Gabizon, A.; Martin, F. Polyethylene Glycol-Coated (Pegylated) Liposomal Doxorubicin. *Drugs* **1997,** *54*, (4), 15-21.
56. Kaminskas, L. M.; Ascher, D. B.; McLeod, V. M.; Herold, M. J.; Le, C. P.; Sloan, E. K.; Porter, C. J. PEGylation of interferon α2 improves lymphatic exposure after subcutaneous and intravenous administration and improves antitumour efficacy against lymphatic breast cancer metastases. *Journal of Controlled Release* **2013,** *168*, (2), 200-208.
57. Moghimi, S. M. The effect of methoxy-PEG chain length and molecular architecture on lymph node targeting of immuno-PEG liposomes. *Biomaterials* **2006,** *27*, (1), 136-144.
58. Yuan, F.; Leunig, M.; Huang, S. K.; Berk, D. A.; Papahadjopoulos, D.; Jain, R. K. Mirovascular Permeability and Interstitial Penetration of Sterically Stabilized (Stealth) Liposomes in a Human Tumor Xenograft. *Cancer Research* **1994,** *54*, (13), 3352-3356.
59. Storm, G.; Belliot, S. O.; Daemen, T.; Lasic, D. D. Surface modification of nanoparticles to oppose uptake by the mononuclear phagocyte system. *Advanced Drug Delivery Reviews* **1995,** *17*, (1), 31-48.
60. Kaminskas, L. M.; Kota, J.; McLeod, V. M.; Kelly, B. D.; Karellas, P.; Porter, C. J. PEGylation of polylysine dendrimers improves absorption and lymphatic targeting following SC administration in rats. *Journal of Controlled Release* **2009,** *140*, (2), 108-116.
61. Abu-Hijleh, M.; Scothorne, R. Regional lymph drainage routes from the diaphragm in the rat. *Clinical Anatomy: The Official Journal of the American Association of Clinical Anatomists and the British Association of Clinical Anatomists* **1994,** *7*, (4), 181-188.
62. Courtice, F.; Harding, J.; Steinbeck, A. The removal of free red blood cells from the peritoneal cavity of animals. *Australian Journal of Experimental Biology and Medical Science* **1953,** *31*, (3), 215-226.
63. Courtice, F.; Steinbeck, A. The lymphatic drainage of plasma from the peritoneal cavity of the cat. *Australian Journal of Experimental Biology and Medical Science* **1950,** *28*, (2), 161-170.
64. Abernethy, N. J.; Chin, W.; Hay, J. B.; Rodela, H.; Oreopoulos, D.; Johnston, M. G. Lymphatic drainage of the peritoneal cavity in sheep. *American Journal of Physiology-Renal Physiology* **1991,** *260*, (3), F353-F358.
65. Flessner, M. F.; Parker, R. J.; Sieber, S. M. Peritoneal lymphatic uptake of fibrinogen and erythrocytes in the rat. *American Journal of Physiology-Heart and Circulatory Physiology* **1983,** *244*, (1), H89-H96.
66. Allen, L.; Vogt, E. A mechanism of lymphatic absorption from serous cavities. *American Journal of Physiology-Legacy Content* **1937,** *119*, (4), 776-782.
67. Parungo, C. P.; Soybel, D. I.; Colson, Y. L.; Kim, S.-W.; Ohnishi, S.; Alec, M.; Laurence, R. G.; Soltesz, E. G.; Chen, F. Y.; Cohn, L. H. Lymphatic drainage of the peritoneal space: a pattern dependent on bowel lymphatics. *Annals of Surgical Oncology* **2007,** *14*, (2), 286-298.
68. Vreim, C.; Ohkuda, K. Improved method for cannulation of the right lymph duct in dogs. *Journal of Applied Physiology* **1977,** *43*, (5), 899-901.
69. Chuang, G. J.-H.; Gao, C.-X.; Mulder, D. S.; Chiu, R. C.-J. Technique of right lymphatic duct cannulation for pulmonary lymph collection in an acute porcine model. *Journal of Surgical Research* **1986,** *41*, (6), 563-568.

70. Shibata, S.; Yamaguchi, S.; Kaseda, M.; Ichihara, N.; Hayakawa, T.; Asari, M. The time course of lymphatic routes emanating from the peritoneal cavity in rats. *Anatomia, histologia, embryologia* **2007,** *36*, (1), 78-82.
71. Shibata, S.-j.; Hiramatsu, Y.; Kaseda, M.; Chosa, M.; Ichihara, N.; Amasaki, H.; Hayakawa, T.; Asari, M. The time course of lymph drainage from the peritoneal cavity in beagle dogs. *Journal of Veterinary Medical Science* **2006,** *68*, (11), 1143-1147.